



FAPI PET: Fibroblast Activation Protein Inhibitor Use in Oncologic and Nononcologic Disease

Yuriko Mori, MD • Katharina Dendl, BS • Jens Cardinale, PhD • Clemens Kratochwil, MD • Frederik L. Giesel, MD, MBA* • Uwe Haberkorn, MD*

From the Department of Nuclear Medicine, Medical Faculty of Heinrich Heine University, University Hospital Düsseldorf, Düsseldorf, Germany (Y.M., K.D., J.C., F.L.G.); Department of Nuclear Medicine, University Hospital Heidelberg, Im Neuenheimer Feld 400, 69120 Heidelberg, Germany (K.D., J.C., C.K., F.L.G., U.H.); and Clinical Cooperation Unit Nuclear Medicine, German Cancer Research Center (DKFZ), Heidelberg, Germany (F.L.G., U.H.). Received April 14, 2022; revision requested June 1; final revision received August 30; accepted September 1. Address correspondence to U.H. (email: uwe.haberkorn@med.uni-heidelberg.de).

* F.L.G. and U.H. are co-senior authors.

Conflicts of interest are listed at the end of this article.

Radiology 2023; 306(2):e220749 • <https://doi.org/10.1148/radiol.220749> • Content codes:  

Gallium 68 (⁶⁸Ga)-labeled fibroblast activation protein (FAP) inhibitor (FAPI) PET is based on the molecular targeting of the FAP, which is known to be highly expressed in the major cell population in tumor stroma, termed cancer-associated fibroblasts. Among many FAP-targeted radiopharmaceuticals developed so far, ⁶⁸Ga-FAPI exhibits rapid tracer accumulation in target lesions and low background signal, which results in excellent imaging features. FAPI PET can be integrated in the clinical workflow and enables the detection of small primary or metastatic lesions, especially in the brain, liver, pancreas, and gastrointestinal tract due to the low tracer accumulation in these organs. Moreover, the DOTA (1,4,7,10-tetraazacyclododecane-1,4,7,10-tetrayl tetraacetic acid) chelator in the molecular structure allows coupling of the FAPI molecules with therapeutic emitters such as yttrium 90 for theranostic applications. This review provides an overview of the state of the art in FAP imaging, summarizes the current knowledge of relevant cancer biology, and highlights the latest findings in the clinical use of ⁶⁸Ga-FAPI PET and other current FAPI tracers.

Published under a CC BY 4.0 license

Fibroblast activation protein (FAP) inhibitor (FAPI) used for PET imaging is a strategy that targets the cell population in the tumor surrounding stroma, termed cancer-associated fibroblasts. Though heterogeneous in origin, cancer-associated fibroblasts can be identified by the upregulation of several surface markers, of which the FAP, a membrane-bound type 2 serine protease belonging to the dipeptidyl peptidase 4 family, represents the most specific surface marker. There have been a few approaches to effectively target this molecule with radiolabeled ligands (eg, antibodies, peptides, or small molecule inhibitors). Among the FAP-based radiotracers developed so far, gallium 68 (⁶⁸Ga)-labeled FAPIs provide the most favorable imaging features in terms of high detection rate in a variety of tumors, even in cases considered to be challenging for conventional fluorine 18 (¹⁸F) fluorodeoxyglucose (FDG) PET. Activation of fibroblasts occurs not only in the tumor surrounding tissue but also under benign conditions such as in wound healing, inflammation, or ischemia. Thus, FAPI PET imaging may also have potential to depict several common benign disease processes that are associated with widespread morbidity.

Background Biology: Activated Fibroblasts in Tumor Stroma

Tumor Stroma and/or Tumor Microenvironment in Oncology

In recent years, the tumor microenvironment has gained growing attention in the context of universal diagnostic and therapeutic strategies in oncology (1,2).

Tumor stroma is reported to develop around malignant cells exceeding a size of 1–2 mm, which provides the basis for visualizing this phenomenon with FAP-targeting strategies (3). The tumor microenvironment is characterized by the abundance of cellular and noncellular components, including fibroblasts, vascular and immune cells, and the extracellular matrix. Increasing evidence suggests that the stroma is the site of a complex crosstalk between neoplastic and nonneoplastic cells, playing a crucial role in tumor development and growth. Multiple growth factors and angiogenic factors secreted from stromal cells, such as transforming growth factor β , vascular endothelial growth factor, interleukin 6, or tumor necrosis factor α lead to the upregulation of oncogenes as well as pro-oncogenic factors and enhance cancer metabolism (3). The tumor microenvironment appears not only to provide mechanical and nutritional support to the malignant cells but also to be fundamentally involved in tumor progression, invasion, metastasis, immunosurveillance, and drug resistance (2,3) (Fig 1).

Cancer-associated Fibroblasts as the Target Cell Population

Cancer-associated fibroblasts constitute the major subpopulation of cells in the tumor stroma (2,3). They are reactive fibroblasts, originating from a variety of benign cells including fibroblasts, adipocytes, endothelial cells, and others. The fibroblasts are activated via stimuli-like hypoxia or oxidative stress to release growth factors. In the course of activation, fibroblasts are transformed from spindle shape into stellate or cells,

Abbreviations

FAP = fibroblast activation protein, FAPI = FAP inhibitor, FDG = fluorodeoxyglucose, SUV_{max} = maximum standardized uptake value, TBR = tumor-to-background ratio



Summary

Gallium 68–labeled fibroblast activation protein inhibitor PET is an oncologic imaging strategy based on the molecular targeting of fibroblast activation protein highly expressed in the stroma of epithelial tumors.

Essentials

- Gallium 68 (^{68}Ga)–labeled fibroblast activation protein (FAP) inhibitor (FAPI) for PET imaging is a radiotracer that can help detect small primary or metastatic lesions in crucial organs like the brain, liver, pancreas, and gastrointestinal tract.
- ^{68}Ga -FAPI PET is especially useful for tumors with a strong desmoplastic reaction, such as breast, colon, and pancreatic cancers, as well as peritoneal carcinomatosis, which show high lesion uptake with sharp image contrast.
- The most widely used ^{68}Ga -labeled FAPIs (eg, ^{68}Ga -FAPI-04, FAPI-74) and further developed FAP–targeting peptides are characterized by rapid and stable tracer accumulation in target lesions.
- DOTA chelator in the molecular structure allows coupling of the FAPI molecules with therapeutic emitters such as lutetium 177 and yttrium 90 for theranostic applications.
- Wound healing, fibrosis (liver, kidney, lung), and inflammation (eg, rheumatoid arthritis, Crohn disease, atherosclerosis, myocardial ischemia) can also be visualized using ^{68}Ga -FAPI PET.

expressing several surface markers such as α -smooth muscle actin, platelet-derived growth factor β , or FAP, which seems to be the most specifically upregulated surface protein (3). Cancer-associated fibroblasts are found in numerous tumors, especially in cancers with strong desmoplastic reactions such as breast, colorectal, pancreatic, prostate, and lung cancer. Accordingly, FAP expression is found in more than 90% of epithelial tumors. As of now, the FAP expression is reported to be associated with a worse prognosis, as shown in colorectal, pancreatic, hepatocellular, and ovarian cancer (1). Although more studies are needed, this aspect makes cancer-associated fibroblasts an attractive target for antitumor therapy. In practical use, the low expression of FAP in quiescent fibroblasts or in healthy adult tissues is beneficial for selective imaging of pathologic changes with low background signal. To note, similar cellular activities occurring in the tumor microenvironment are also observed in wound healing or inflammatory tissue process, providing the basis for visualizing those nonmalignant conditions with the same imaging procedure.

Targeting FAP

The development of imaging techniques requires molecules with selective tracer binding and a rapid, high rate of radioligand uptake and fast clearance from circulation. Among the FAP tracers developed so far, ^{68}Ga -FAPIs provide the most favorable features, mostly fulfilling the above-mentioned demands with increasing clinical evidence.

FAP Characteristics

FAP is a membrane-anchored glycoprotein consisting of 760 amino acids with a short intracellular (six amino acids), transcellular (20 amino acids), and a large extracellular (734 amino acids) domain (4). FAP belongs to the dipeptidyl peptidase family, the most familiar protein being dipeptidyl peptidase IV, also known as CD26, with which FAP shares up to 48% of the amino acid sequence. FAP characteristically possesses both postproline peptidase and endopeptidase activity, enabling FAP to cleave proteins in the surrounding tissue, thus promoting protein degradation and matrix remodeling.

FAPI Tracers

The main challenge to obtain therapeutic efficacy with clinical tolerability was notably overcome with tracers based on enzyme inhibition. Jansen et al (61) proposed several small enzyme inhibitors specific for FAP, including UAMC-1110 with increased specificity for FAP. Through the chemical modification of the quinoline group of UAMC-1110, resulting in the successful attachment of different chelators, Lindner et al (5) were the first to synthesize ^{68}Ga -labeled FAPIs with specific binding to FAP, which presented a rapid and almost complete internalization of the ligand-receptor complex (Fig 2). Subsequent dosimetric analysis comparing ^{68}Ga -FAPI-02 and -04 in patients revealed a favorable equivalent dose of approximately 3–4 mSv for 200 MBq of both radiopharmaceuticals, which is comparable to ^{18}F -FDG or ^{68}Ga DOTA-(Tyr3)-octreotate (DOTATATE) (6). Further improvement in tumor-to-background ratios (TBRs) with higher image contrast was achieved, especially for ^{68}Ga -FAPI-21 and -46 (7). In particular, ^{68}Ga -FAPI-46 showed an increasing TBR over time, making this tracer a promising tool for future theranostic applications.

Recent Approaches

Other recent approaches to target FAP are based on peptide or peptidomimetic compounds. OncoFAP (Philogen) is a small organic FAP ligand with ultrahigh affinity (8). [^{68}Ga]Ga-OncoFAP DOTA-GA anhydride (DOTAGA) is reported to bind to human FAP in a subnanomolar concentration range, with rapid tracer accumulation and low immunogenicity due to its low molecular weight (9). The tracer accumulation profile of 10 minutes to 3 hours after administration is comparable to that of [^{68}Ga]Ga-FAPI-04. Its clinical use after radiolabeling with therapeutic emitters will be the subject of future investigations.

Cancer Imaging with ^{68}Ga -FAPI PET

FDG versus FAPI

Although ^{18}F -FDG is currently the most widely used radiotracer for PET imaging in oncology, it has substantial disadvantages for a variety of applications. Nonspecific and physiologic radiotracer uptake in crucial organs reduces the diagnostic accuracy in many cases. FAPI PET is indepen-

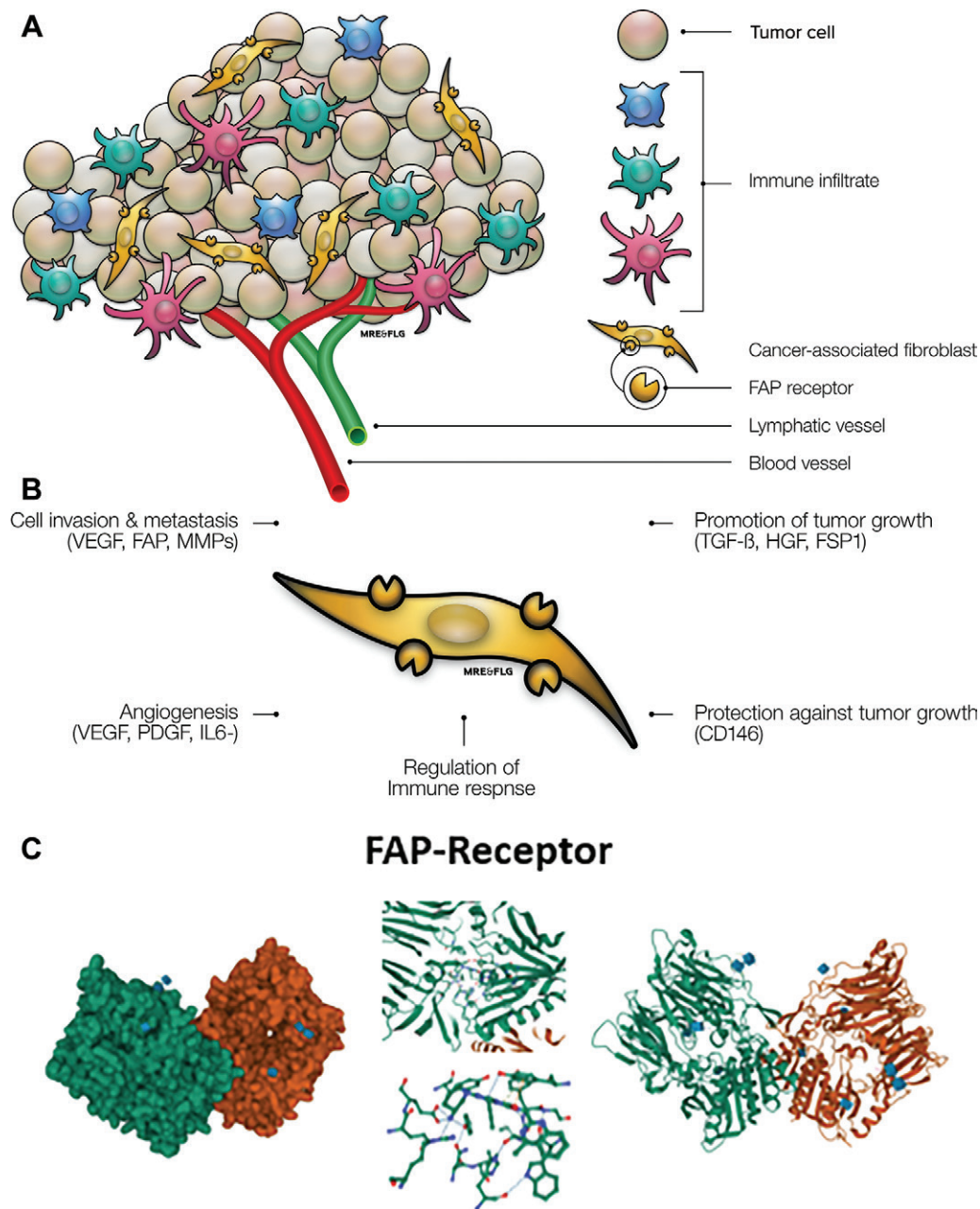


Figure 1: Illustrations of tumor environment. **(A)** Neoplastic tissue and, therefore, the tumor microenvironment comprise a variety of components apart from cancer cells alone. When reaching a size of 2–3 mm, the tumor-associated stroma plays a crucial role in growth and progression, and it may even contribute up to 90% of the malignant mass. The tumor stroma mainly consists of the basement membrane, immune cells, vascular network, and cancer-associated fibroblasts. **(B)** Cancer-associated fibroblasts are responsible for vital processes of malignant tumors. Through different transmitters and pathways, cancer-associated fibroblasts enhance cell invasion and promotion of metastases. Simultaneously, they facilitate tumor growth, enable angiogenesis, and influence immune responses. Already these few features undermine the importance of cancer-associated fibroblasts regarding malignant tumors and their potential for diagnostic and therapeutic implications. **(C)** Gaussian surface (left) and fibroblast activation protein (FAP) receptor (right). The illustrations in the middle show the interaction of relevant amino acids within FAP receptor with its ligand linagliptin. FSP1 = fibroblast-specific protein, HGF1 = hepatocyte growth factor, IL6 = interleukin 6, MMP = matrix metalloproteases, PDGF = platelet-derived growth factor, TGF- β = transforming growth factor β , VEGF = vascular endothelial growth factor. Images were generated using data sets 1Z68 and 6Y0F from references 59 and 60.

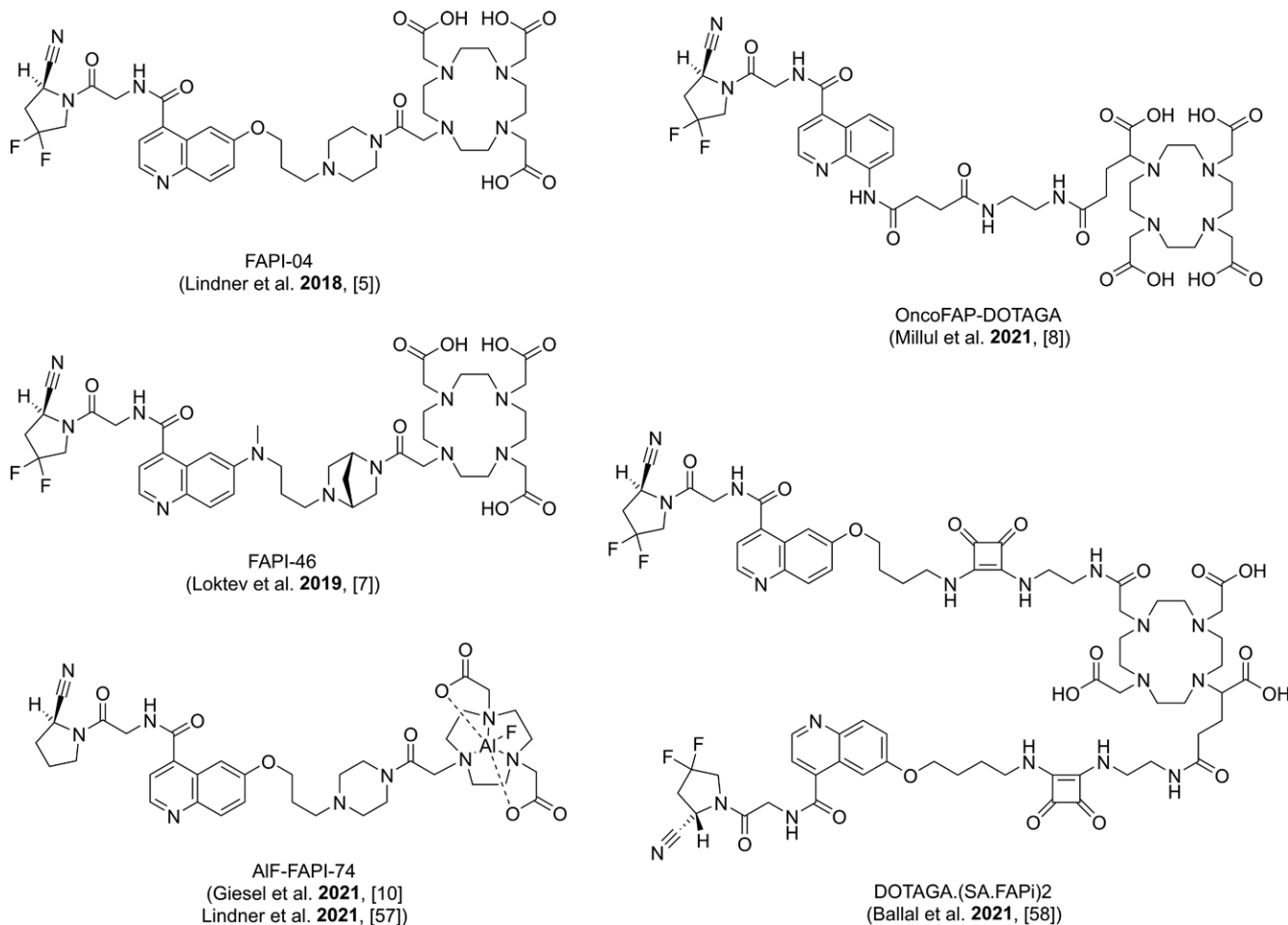


Figure 2: Overview of advanced fibroblast activation protein (FAP) ligands. All depicted FAP ligands share a highly similar pharmacophore and/or FAP-binding domain. AIF-FAPI-74 is a pure diagnostic FAP inhibitor and can be labeled with fluorine 18 (or gallium 68 [^{68}Ga]). The remaining FAP ligands are all capable of binding theranostic radionuclides like ^{68}Ga , lutetium 177, yttrium 90, samarium 153, and actinium 225 via their DOTA (1,4,7,10-tetraazacyclododecane-1,4,7,10-tetrayl tetraacetic acid) or DOTAGA (DOTA-GA anhydride) chelator.

dent of glucose activity, leading to the drastic reduction of background signal in the brain, liver, oro- and nasopharyngeal mucosa, or gastrointestinal tract. In practical use, ^{68}Ga -FAPI can be used without any dietary preparation and provides stable tracer uptake 10 minutes to 3 hours after administration. ^{18}F -labeled FAP ligands such as FAPI-74 allow a larger batch production with lower costs (10). Considering the favorable organ distribution and high image quality, ^{18}F -FAPI-74 possesses the potential to outperform FDG. Furthermore, phase 2 studies have been recently initiated—particularly in the field of oncologic PET imaging.

A broad overview of the larger studies reveals superior performance for FAPI PET, especially in the detection of primary or metastatic liver lesions and pancreatic, gastric, colon, lung, and ovarian cancers (11–14) (Figs 3, 4). Peritoneal carcinomatosis is an entity increasingly mentioned in many studies for showing clear superiority over FDG, as in a targeted study encompassing 46 patients with peritoneal carcinomatosis (15). In different metastatic lesions, an overall high detection rate was found for lymph nodes, bone, lung,

and visceral metastasis in larger studies, leading to changes in clinical staging (Fig 5). Although the documented intensity of the uptake value has varied for each tumor entity in subsequent studies, suspicious lesions are easily found because of the substantially low background signal, which leads to a high TBR with sharp image contrast (Fig 6).

Organ- and Tumor-specific Studies: Cancers for which FAPI is Superior to FDG

Organ- and tumor-specific studies reveal more details, especially regarding diagnostic performance compared with other imaging modalities (Table 1).

Glioblastoma.—Röhrich et al (33) first found in 2019 the elevated FAPI uptake and TBR in isocitrate dehydrogenase (IDH)–wildtype glioblastomas (maximum standardized uptake value [SUV_{max}], 4.2; TBR, 22.4) and grade III or IV, but not in grade II, IDH-mutant gliomas (SUV_{max} , 0.4; TBR, 1.8). Based on this finding, the authors concluded that FAPI PET allows noninvasive distinction between low-grade IDH-mutant and high-grade

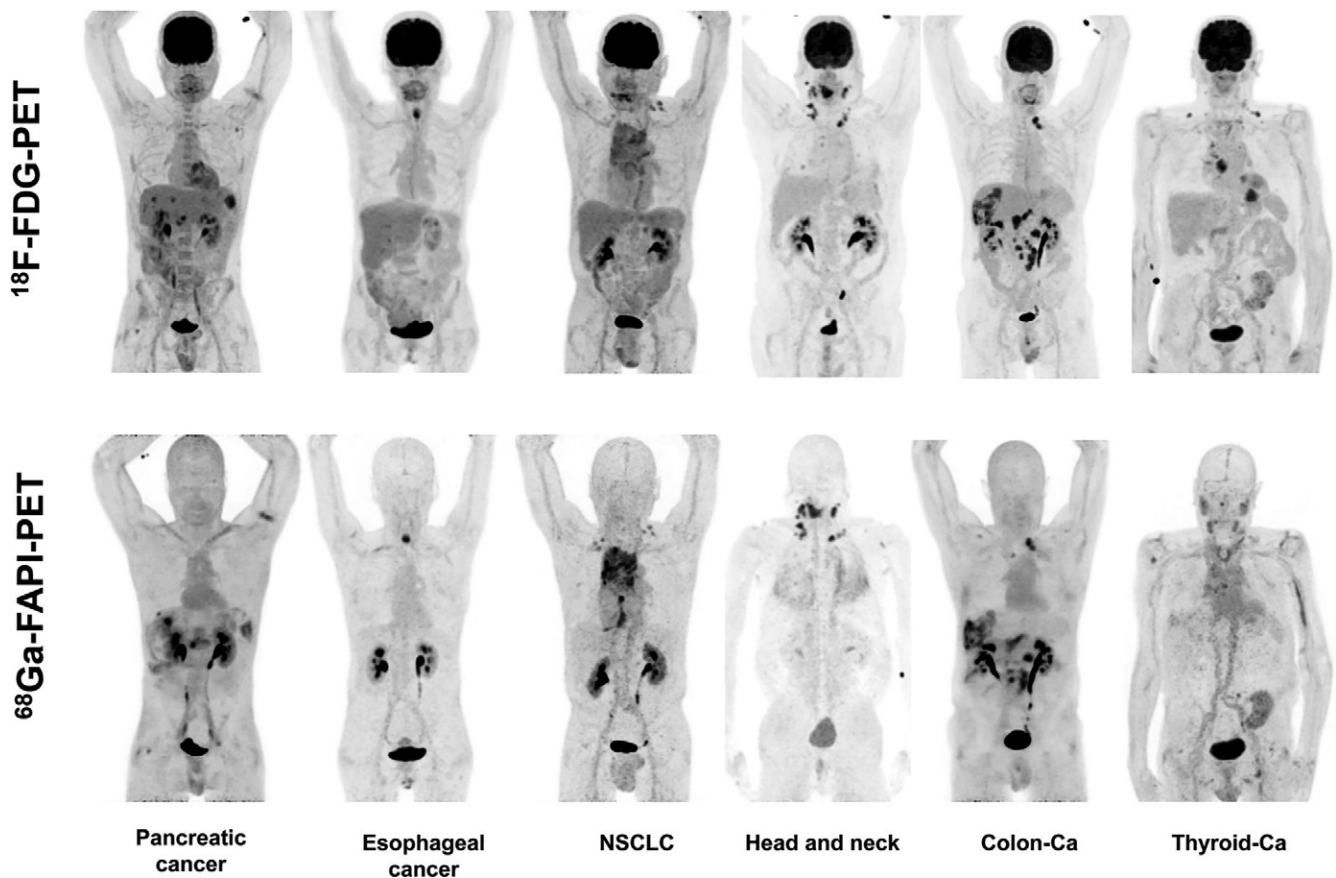


Figure 3: Intraindividual comparison of fluorodeoxyglucose (FDG) versus fibroblast activation protein inhibitor (FAPI) PET in cancer. Images were obtained in six patients with six different tumor entities who underwent fluorine 18 (^{18}F) FDG PET and gallium 68 (^{68}Ga) FAPI PET within fewer than 9 days. Five of the six patients show similar strong tumor uptake with ^{18}F -FDG and ^{68}Ga -FAPI, and three of six could benefit from a lower background signal in the liver or pharyngeal mucosa. In contrast, the patient with iodine-negative thyroid cancer showed only minor ^{68}Ga -FAPI tracer uptake compared with ^{18}F -FDG. Ca = cancer, NSCLC = non-small cell lung cancer. (Adapted, under a CC BY license, from reference 6.)

gliomas. Windisch et al (34) investigated glioblastoma for radiation therapy planning. They found that FAPI PET for target volume delineation resulted in gross tumor volumes containing tumor not covered by MRI gross tumor volume.

Nasopharyngeal carcinoma.—For nasopharyngeal carcinomas, Qin et al (35) showed lower SUV_{max} of primary tumors in FAPI (13.9 ± 5.1) than in FDG (17.7 ± 6.8). The same authors found that FAPI PET improved the delineation of skull base and intracranial invasion.

Head and neck cancer.—Syed et al (36) demonstrated in 14 patients with head and neck cancer high FAPI avidity in primary tumors (SUV_{max} , 14.6 ± 4.4) without comparison to FDG. With regard to radiation therapy planning, the same study showed that contouring with FAPI resulted in significantly larger gross tumor volume with three- and fivefold increase in FAPI enhancement as compared with CT-based gross tumor volume. Head and neck cancers of unknown primary tumor were investigated by Gu et al (37) in patients without any findings at FDG PET. FAPI PET depicted the primary tumor in seven of 18 patients (39%).

Moderate to intense FAPI uptake (mean SUV_{max} , 8.8) and TBR of 4.5 were found in primary tumors (37).

Prostate cancer.—Kessel et al (38) showed in a study including six patients with metastatic castration-resistant prostate cancer the variable FAPI uptake ranging from 5.7 to 27.8 (38). Thus, FAPI PET as well as FDG PET might be used as a complementary imaging modality to prostate-specific membrane antigen PET for prostate cancer, particularly in tumors with a higher Gleason score.

Organ- and Tumor-specific Studies: Cancer Entities without Superiority of FAPI over FDG

Lymphoma.—Jin et al (39) demonstrated in a study including 11 patients with Hodgkin lymphoma and 62 with non-Hodgkin lymphoma an overall SUV_{max} of 9.5 ± 4.6 for FAPI PET/CT, with no difference in nodal and extranodal lesions ($P > .05$).

Multiple myeloma.—Elboga et al (40) found no significant superiority of FAPI PET/CT over FDG PET/CT in a study including 14 patients with multiple myeloma.

Comparison of FAPI vs. FDG in oncological PET-imaging

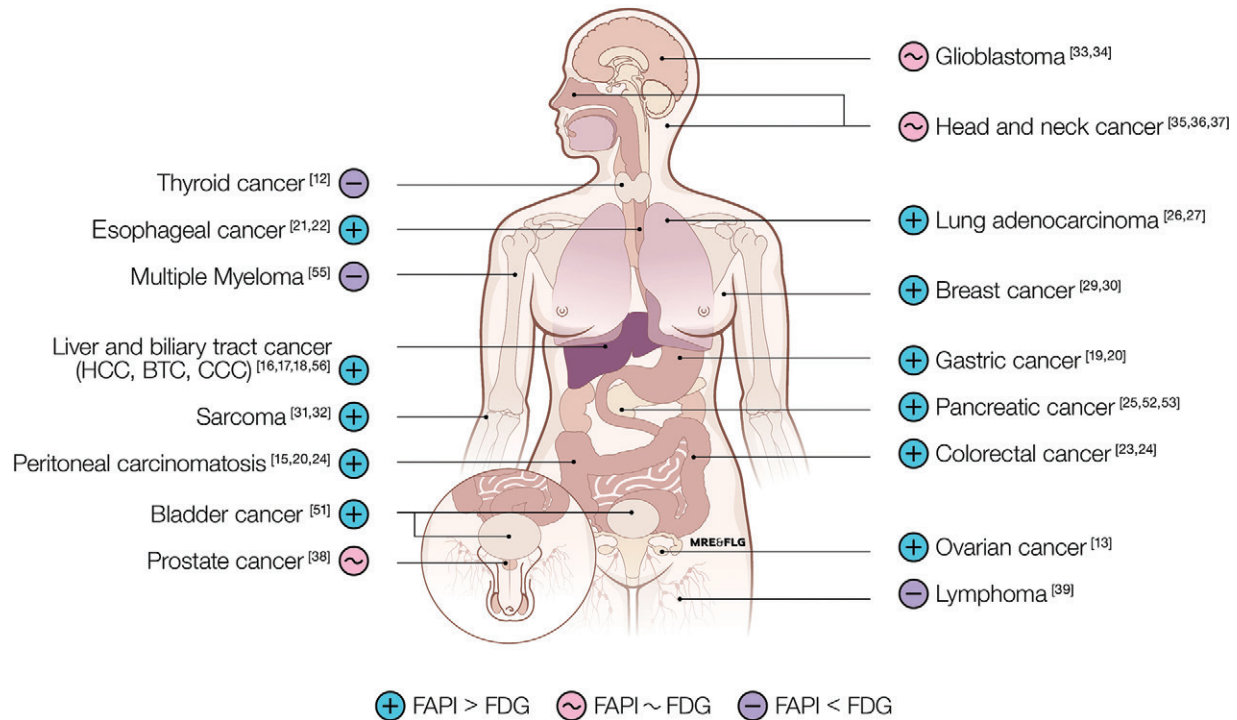


Figure 4: Fibroblast activation protein inhibitor (FAPI) versus fluorodeoxyglucose (FDG) PET in various cancer entities. Diagram shows comparison of FAPI and FDG PET in the diagnostic characteristic of various cancer entities based on the current studies (reference numbers are in brackets). BTC = biliary tract cancer, CCC = cholangiocellular carcinoma, HCC = hepatocellular carcinoma.

Theranostic Applications

The initial theranostic application of FAP-based radiotracers was performed using yttrium 90 (^{90}Y)-FAP-04 as reported by Lindner et al (5). In that study, 2.9 GBq of the therapeutic radiotracer was applied in a patient with metastasized breast cancer with good tolerability, leading to a substantial reduction of pain medication (5). Further successful clinical application was reported for ^{90}Y - and samarium 153-labeled FAPI-46 (41–43). Although more evidence is needed, multiple results in preclinical and clinical settings (eg, with actinium 225-labeled FAPI-04) suggest a potential of FAP tracers for a future theranostic application (43). An overview of the major FAP tracers for diagnostic and theranostic use is given in Table 2.

Noncancer Imaging

“Wounds That Do Not Heal”

Matrix remodeling and tissue repair are typically seen in benign conditions such as wound healing. Dvorak originally referred to tumors in this context as “wounds that do not heal” (2). Activated fibroblasts are found in scar formation (eg, in ischemic tissues after myocardial infarction), chronic inflammatory and/or destructive processes (rheumatoid arthritis, Crohn disease, atherosclerotic plaque, immunoglobulin G4-related diseases), fibrosis (liver, kidney, lung), and

benign tumors. These are conditions that clinicians must be aware of for the correct interpretation of the acquired image with FAP-targeting tracers. On the other hand, if properly used, FAP-targeting tracers provide the effective noninvasive diagnostic strategy for the aforementioned diseases.

Cardiac Imaging with FAP

In one preclinical study, the uptake of (^{68}Ga)Ga-FAPI-04 in the injured myocardium peaked on day 6 after acute myocardial infarction (44). In addition, in a retrospective patient study, an intense FAPI uptake was observed in the infarct region (45). Interestingly, in that study, the corresponding cardiac MRI scan revealed that regions with positive FAPI uptake were slightly larger than the pathologic changes seen at cardiac MRI, indicating that the FAPI-positive areas might include the adjacent viable zone. Another finding relevant for clinical use is that the previous infarct area detected at cardiac MRI showed no tracer uptake at FAPI PET. This is presumably due to the substantial reduction of activated fibroblasts during scar maturation and provides a basis for the possible differentiation between fresh and matured ischemia.

Liver, Kidney, and Lung Fibrosis

In the kidney, a significant correlation of FAPI uptake with the deteriorated kidney function was recently shown and

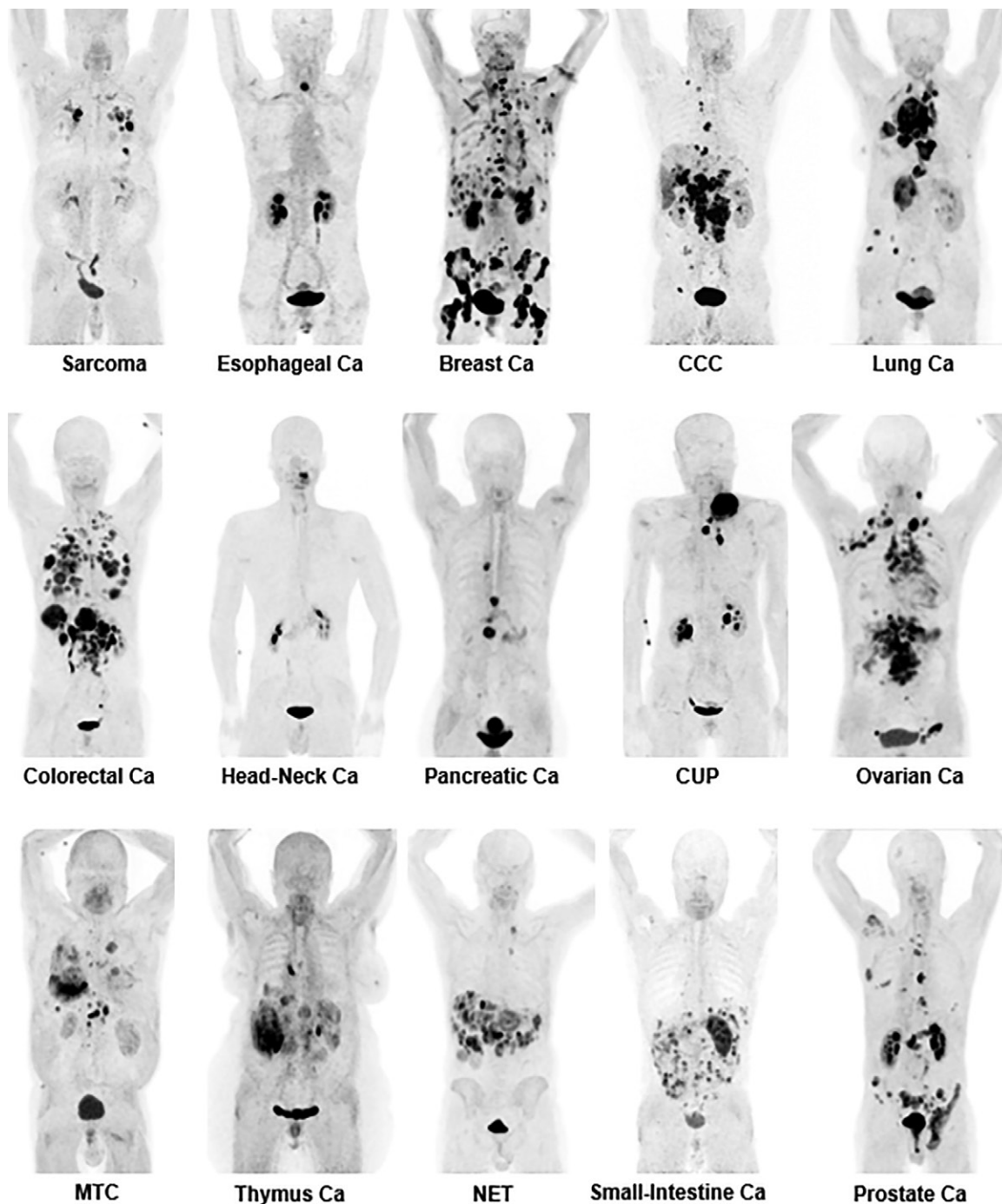


Figure 5: Fibroblast activation protein inhibitor (FAPI) PET/CT scans of various cancer entities. Maximum intensity projections in several patients undergoing FAPI PET/CT include a variety of different tumor entities. Ca = cancer, CCC = cholangiocellular carcinoma, CUP = cancer of unknown primary, MTC = medullary thyroid carcinoma, NET = neuroendocrine tumor. (Adapted, under a CC BY license, from reference 12.)

confirmed by another study (46). Idiopathic pulmonary fibrosis is more challenging to diagnose than kidney fibrosis due to the absence of suitable surface markers for disease monitoring. In a preclinical trial, FAPI PET showed a promising result with significantly higher tracer uptake in bleomycin-induced fibrotic lung of mice (47). Another recent report on [^{68}Ga]Ga-FAPI-46–positive and ^{18}F -FDG–

negative findings in the lung after COVID-19 infection suggests the potential efficacy of FAPI PET in the evaluation of fibrous changes in the infectious or postinfectious lung (48). For liver fibrosis, elevated FAP expression in hepatic stellate cells was identified in the periseptal areas of the cirrhotic liver, indicating the efficacy of using FAPI PET for the assessment of active fibrosis (49).

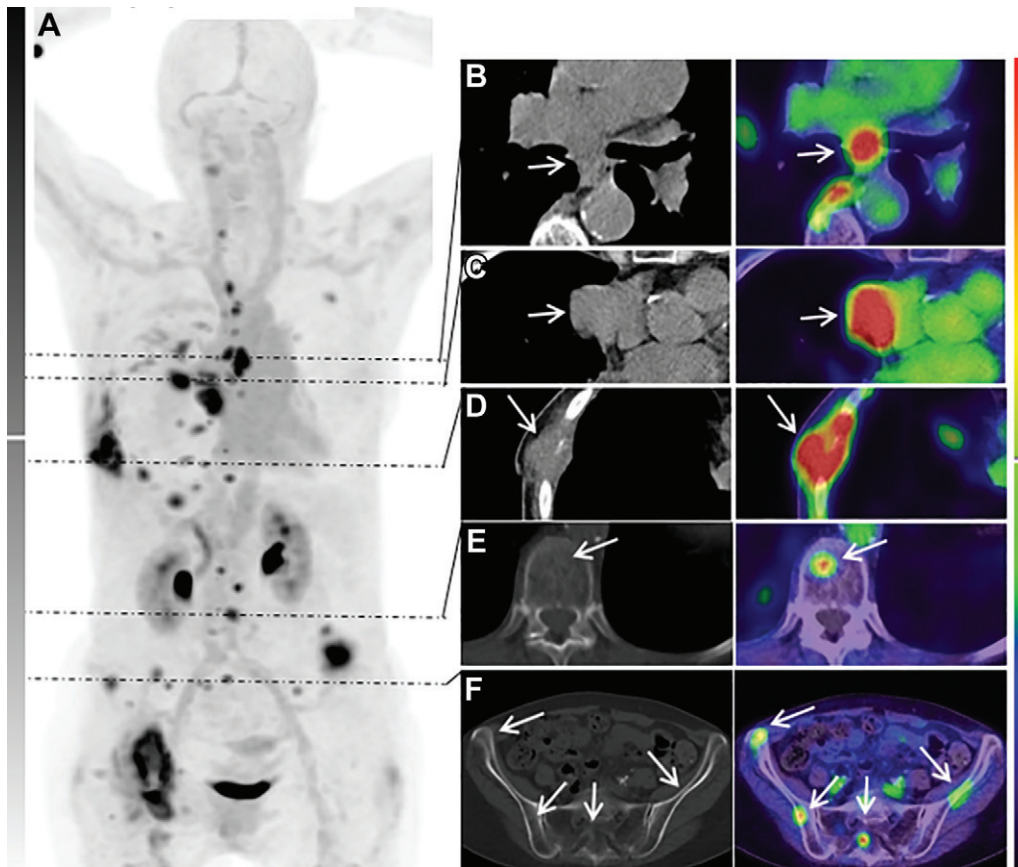


Figure 6: Image obtained in a 61-year-old man with newly diagnosed squamous cell carcinoma of the lung for initial tumor staging. **(A)** Maximum intensity projection of fluorine 18 (^{18}F) fibroblast activation protein inhibitor (FAPI)-74 PET scan shows the wide distributions of tumor metastases. **(B–F)** CT scans (left) and axial fused FAPI PET/CT images (right). **(C)** Axial fused FAPI PET/CT scan enables favorable discrimination between tumor (arrows) and myocardium. **(B, D)** Some fibroblast activation protein–positive lesions (arrows) were confirmed with CT correlate (left images), whereas additional bone lesions (arrows) were only detected with FAPI PET **(E, F, right image)**. All arrows represent FAPI uptake with morphologic correlation. (Adapted, under a CC BY license, from reference 10.)

Other FAP-positive Benign Conditions

In chronic inflammation, intestinal myofibroblasts play a key role in sustaining diseases, promoting fibroproliferative and stenotic changes. In Crohn disease, the elevated FAP expression was observed in areas with stricture (50). Interestingly, these changes were mostly absent in ulcerative colitis, providing the possibility for noninvasive differentiation of the two diseases.

Further FAP-positive findings with future potential for diagnostic use are immunoglobulin G4–related diseases, rheumatoid arthritis, atherosclerotic plaque, and checkpoint inhibitor–associated myocarditis.

Conclusion

Fibroblast activation protein inhibitor PET has diagnostic and therapeutic potential in oncology and even beyond. Future studies are needed for more evidence in each tumor entity, as well as the careful validation of nonmalignant conditions for the correct interpretation of the acquired images.

Acknowledgments: We highly appreciate the support of Mike Reiss, Dipl Ing, for graphical design and illustration and Emil Novruzov, MD, for additional proofreading.

Disclosures of conflicts of interest: Y.M. No relevant relationships. K.D. No relevant relationships. J.C. No relevant relationships. C.K. Royalties from SOFIE Biosciences and iTheranostics; patents in the field of PSMA, FAP inhibitors; participates on advisory board on neuroendocrine tumors for Advanced Accelerator Applications Germany, a Novartis company; stock or stock options in FAPi-Holding. F.L.G. FAPI co-inventor; consulting fees from Telix Pharma, SOFIE, ABX, Alpha Fusion; royalties from iTheranostics and SOFIE Biosciences; patent for FAPI tracers licensed to SOFIE Biosciences. U.H. Royalties from iTheranostics and SOFIE Biosciences; patent for FAPI tracers licensed to SOFIE Biosciences.

References

1. Fitzgerald AA, Weiner LM. The role of fibroblast activation protein in health and malignancy. *Cancer Metastasis Rev* 2020;39(3):783–803.
2. Dendl K, Koerber SA, Kratochwil C, et al. FAP and FAPI-PET/CT in Malignant and Non-Malignant Diseases: A Perfect Symbiosis? *Cancers (Basel)* 2021;13(19):4946.
3. Loktev A, Lindner T, Mier W, et al. A Tumor-Imaging Method Targeting Cancer-Associated Fibroblasts. *J Nucl Med* 2018;59(9):1423–1429.
4. Zi F, He J, He D, Li Y, Yang L, Cai Z. Fibroblast activation protein α in tumor microenvironment: recent progression and implications (review). *Mol Med Rep* 2015;11(5):3203–3211.

Table 1: Organ- and Tumor-specific Studies with FAPI PET

Organ and Tumor Type	Imaging Modality	Study and Year	No. of Patients
Brain			
IDH-wild type glioblastoma and/or grade III or IV IDH-mutant glioma	FAPI PET/CT	Röhrich et al 2019 (33)	18
Glioblastoma	FAPI PET/CT and CE CT or MRI	Windisch et al 2020 (34)	12
Head and neck			
Head and neck cancer	FAPI PET/CT and CE CT or MRI	Syed et al 2020 (36)	14
Head and neck cancer of unknown primary	FDG PET/CT and FAPI PET/CT	Gu et al 2022 (37)	18
Nasopharyngeal carcinoma	FDG PET/CT and FAPI PET/CT	Qin et al 2021 (35)	15
Lung			
Adenocarcinoma and/or squamous cell carcinoma	FAPI PET/CT and CE CT or MRI	Giesel et al 2022 (10)	10
Adenocarcinoma	FDG PET/CT and FAPI PET/CT	Wang et al 2022 (27)	34
Liver			
Hepatocellular and cholangiocellular carcinoma	FDG PET/CT and FAPI PET/CT	Shi et al 2021 (17)	20
Hepatocellular carcinoma	FDG PET/CT and FAPI PET/CT	Wang et al 2021 (16)	29
Hepatocellular and cholangiocellular carcinoma	FDG PET/CT, FAPI PET/CT, and CE CT or MRI	Guo et al 2020 (18)	34
Biliary tract			
Biliary tract cancer	FDG PET/CT and FAPI PET/CT	Lan et al 2022 (56)	18
Gastrointestinal tract and/or peritoneum			
Esophageal cancer	FDG PET/CT, FAPI PET/CT, and CE CT or MRI	Zhao et al 2021 (21)	21
Esophageal cancer	FAPI PET/CT and CE CT or MRI	Ristau et al 2020 (22)	7
Gastric cancer	FDG PET/CT and FAPI PET/CT	Qin et al 2021 (20)	20
Gastric cancer	FDG PET/CT and FAPI PET/CT	Kuten et al 2021 (19)	13
Colorectal and anal cancer	FAPI PET/CT and CE CT or MRI	Koerber et al 2020 (23)	22
Gastric, duodenal, and colorectal cancer	FDG PET/CT and FAPI PET/CT	Pang et al 2021 (24)	35
Peritoneal carcinomatosis	FDG PET/CT and FAPI PET/CT	Pang et al 2021 (24)	11*
Peritoneal carcinomatosis	FDG PET/CT and FAPI PET/CT	Zhao et al 2021 (15)	46
Peritoneal carcinomatosis	FDG PET/CT and FAPI PET/CT	Qin et al 2021 (20)	10*
Pancreas			
Pancreatic cancer	FDG PET/CT, FAPI PET/CT, and CE CT or MRI	Pang et al 2022 (25)	36
Pancreatic cancer	FAPI PET/CT and CE CT or MRI	Liermann et al 2021 (52)	7
Pancreatic cancer	FAPI PET/CT and CE CT or MRI	Röhrich et al 2021 (53)	19
Soft tissue			
Sarcoma	FDG PET/CT and FAPI PET/CT	Kessler et al 2021 (32)	47
Sarcoma	FAPI PET/CT	Koerber et al 2021 (31)	15
Gynecologic tumors			
Ovarian cancer	FDG PET/CT and FAPI PET/CT	Dendl et al 2021 (13)	9*
Breast cancer	FDG PET/CT and FAPI PET/CT	Elboga et al 2021 (30)	48
Breast cancer	FDG PET/CT and FAPI PET/CT	Kömek et al 2021 (29)	20
Urinary tract and/or prostate			
Bladder cancer	FDG PET/CT and FAPI PET/CT	Novruzov et al 2022 (28)	8
Prostate cancer	FAPI PET/CT	Kessel et al 2021 (38)	6
Hematologic disorders			
Lymphoma	FAPI PET/CT	Jin et al 2022 (39)	11
Multiple myeloma	FDG PET/CT and FAPI PET/CT	Elboga et al 2022 (40)	14
Mixed tumor entities			
Various tumors	FAPI PET/CT	Kratochwil et al 2019 (12)	80
Various tumors	FDG PET/CT and FAPI PET/CT	Giesel et al 2019 (6)	50
Various tumors	FDG PET/CT and FAPI PET/CT	Chen et al 2020 (14)	75
Various tumors	FDG PET/CT and FAPI PET/CT	Giesel et al 2021 (11)	71
Various tumors	FDG PET/CT and FAPI PET/CT	Dendl et al 2021 (54)	55
Various tumors	FDG PET/CT and FAPI PET/CT	Chen et al 2021 (55)	68
Various tumors	FDG PET/CT and FAPI PET/CT	Dendl et al 2021 (13)	31

Note.—CE = contrast enhanced, FAPI = fibroblast activation protein inhibitor, FDG = fluorodeoxyglucose, IDH = isocitrate dehydrogenase.

* As part of a larger study.

Table 2: Overview of the Major FAP Ligands

FAP Ligand	Diagnostic Emitter	Therapeutic Emitter	Study	Features
FAPI-02	⁶⁸ Ga	...	Lindner et al (5)	Early small molecule FAP tracer
FAPI-04	⁶⁸ Ga	⁹⁰ Y, ²²⁵ Ac	Lindner et al (5), Watabe et al (43)	First clinically applied small molecule FAP tracer
FAPI-34	^{99m} Tc	¹⁸⁸ Re	Lindner et al (42)	Applied for diagnostic scintigraphy and SPECT, theranostic possible
FAPI-46	⁶⁸ Ga	⁹⁰ Y, ¹⁵³ Sm	Loktev et al (7), Kratochwil et al (41)	Applied for diagnostic PET, potential theranostic applications
FAPI-74	⁶⁸ Ga, ¹⁸ F	...	Giesel et al (10), Lindner et al (57)	Applied for diagnostic PET with ¹⁸ F, potential application with ⁶⁸ Ga
OnkoFAP-DOTAGA	⁶⁸ Ga	...	Backhaus et al (9), Millul et al (8)	Applied for diagnostic PET, considered for theranostic applications
DOTA.SA.FAPI	⁶⁸ Ga	...	Ballal et al (58)	Applied for diagnostic PET
DOTAGA.(SA.FAPI)2	⁶⁸ Ga	¹⁷⁷ Lu	Ballal et al (58)	Applied for diagnostic PET, theranostic application

Note.—²²⁵Ac = actinium 225, ¹⁸F = fluorine 18, FAP = fibroblast activation protein, FAPI = FAP inhibitor, ⁶⁸Ga = gallium 68, ¹⁷⁷Lu = lutetium 177, ¹⁸⁸Re = rhenium 188, ¹⁵³Sm = samarium 153, ^{99m}Tc = technetium 99m, ⁹⁰Y = yttrium 90.

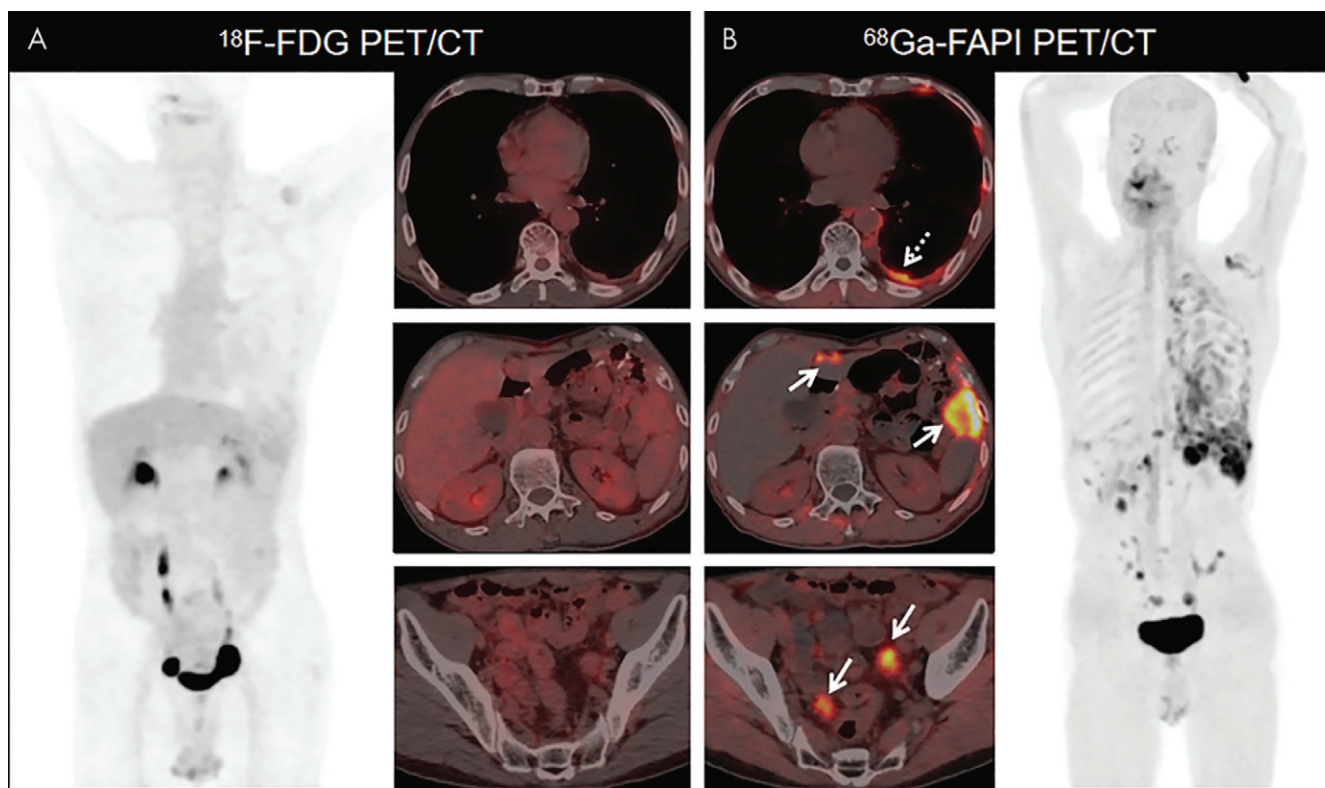


Figure 7: Images in a 66-year-old man who had undergone radical gastrectomy for gastric adenocarcinoma and presented with abdominal pain and rising tumor marker levels. **(A)** Images from fluorine 18 (¹⁸F) fluorodeoxyglucose (FDG) PET/CT show the thickened pleura and multiple nodules in the peritoneum and mesentery, with low-to-moderate ¹⁸F-FDG activity in these lesions (left image: anterior maximum intensity projection image from ¹⁸F FDG PET; right images: axial fused PET/CT images). **(B)** Images from gallium 68 (⁶⁸Ga) fibroblast activation protein inhibitor (FAPI) PET/CT show much higher tracer uptake in the thickened pleura (dashed arrow) and peritoneal nodules (solid arrows) (right image: anterior maximum intensity projection image from FAPI PET; left images: axial fused PET/CT images). Subsequent biopsy of pleura and peritoneal nodules revealed metastatic gastric adenocarcinoma (poorly differentiated). (Reprinted, under a CC BY license, from reference 24.)

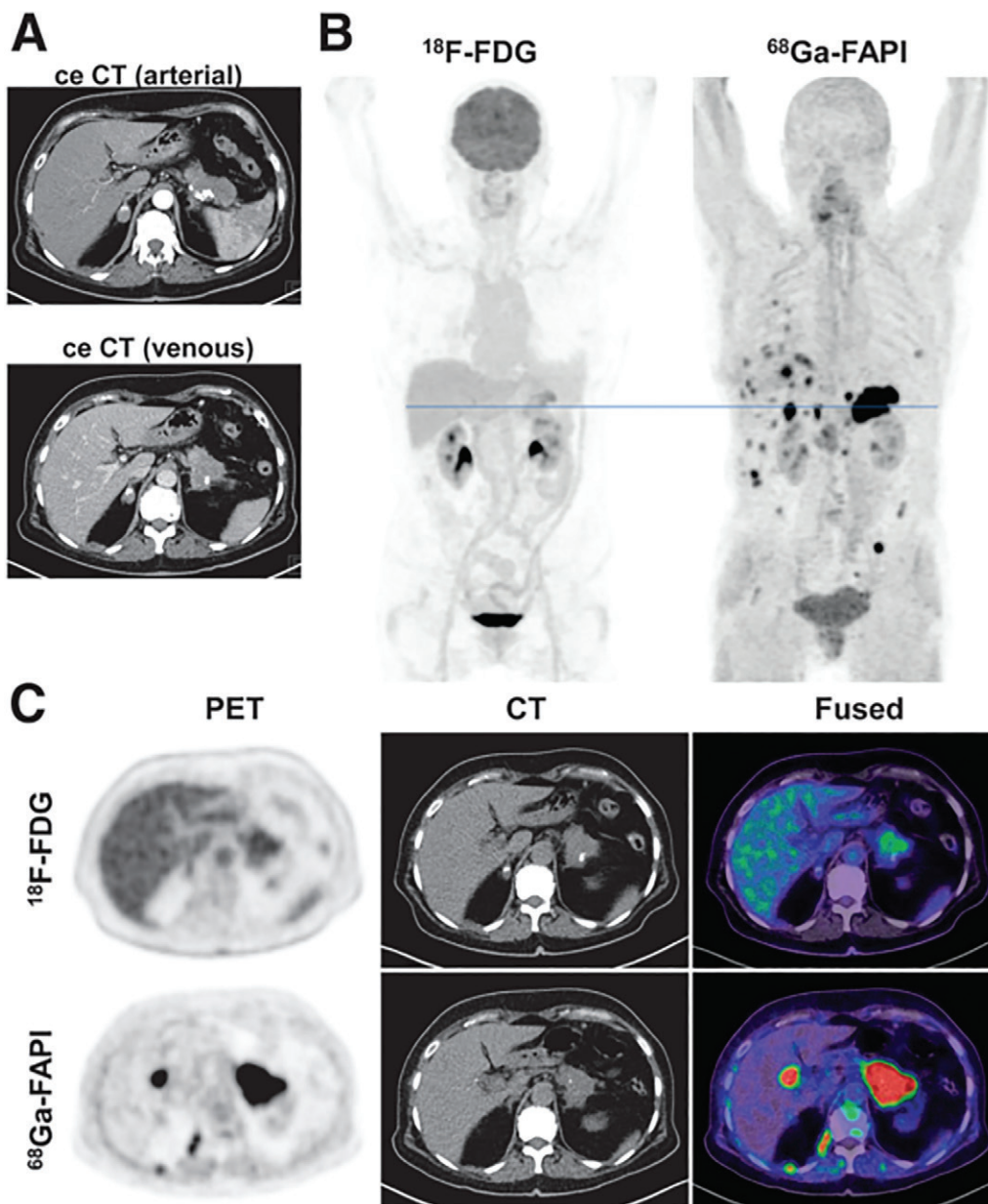


Figure 8: Images obtained for primary staging in a 58-year-old man with pancreatic ductal adenocarcinoma. **(A)** Axial contrast-enhanced (ce) CT images of pancreatic ductal adenocarcinoma and liver in arterial (upper image) and venous (lower image) phase. **(B)** Mean intensity projection images from fluorine 18 (^{18}F) fluorodeoxyglucose (FDG) (left) and gallium 68 (^{68}Ga) fibroblast-activation protein inhibitor (FAPI) (right) PET/CT. **(C)** Axial fused ^{18}F -FDG CT image (upper row, right image) and FAPI PET/CT image (lower row, right image) in the same patient at the level (blue line in **B**) of the pancreatic tumor mass and another suspicious FAPI accumulation in projection on perihepatic lymph node (corresponding CT scans, middle images). A metastatic situation, which had been revealed with FAPI PET/CT, was confirmed with biopsy of pulmonary lesion that was diagnosed as metastasis of known pancreatic ductal adenocarcinoma. (Adapted, under a CC BY license, from reference 53.)

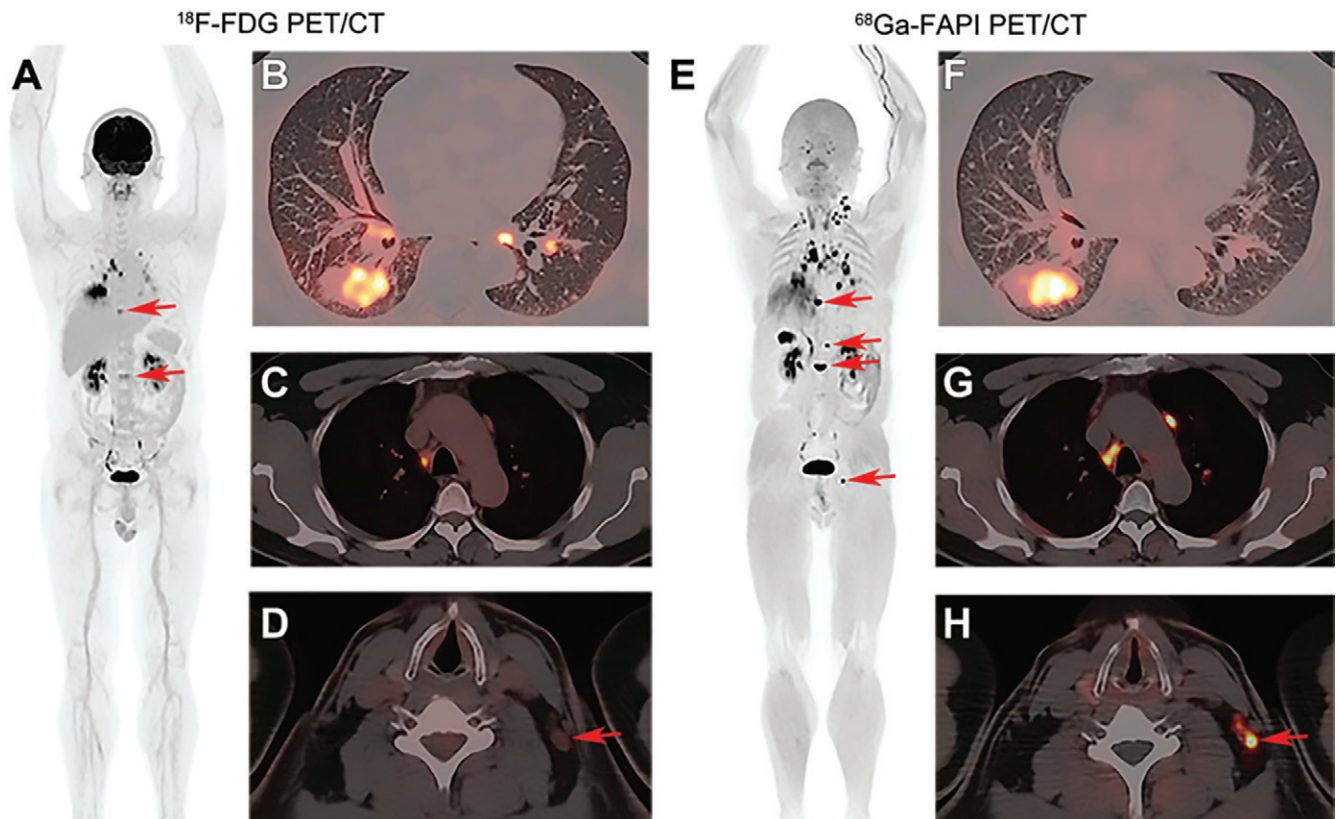


Figure 9: Images in a 46-year-old man with newly diagnosed lung adenocarcinoma for tumor staging. **(A)** Fluorine 18 (^{18}F)-labeled fluorodeoxyglucose (FDG) maximum intensity projection PET image, **(B)** axial fused ^{18}F -FDG PET/CT image of lung, and **(C, D)** axial fused ^{18}F -FDG PET/CT images of mediastinum and neck. **(E)** Gallium 68 (^{68}Ga)-labeled fibroblast activation protein inhibitor (FAPI) maximum intensity projection image, **(F)** axial fused ^{68}Ga -FAPI PET/CT image of the lung, and **(G, H)** axial fused ^{68}Ga -FAPI images of mediastinum and neck. Primary lung cancer (size, 4.9×4.2 cm) in the lower lobe of right lung was detected with intense uptake of ^{18}F -FDG and ^{68}Ga -FAPI (maximum standardized uptake value, 10.4 and 12.4) **(A, B, E, F)**. Multiple small lung metastases were also observed with both techniques **(B, F)**. ^{18}F -FDG PET/CT images show multiple positive lymph nodes in right hilum and mediastinum **(A, C)**. ^{68}Ga -FAPI PET/CT images depict more positive lymph nodes not only in right hilum and mediastinum **(E, G)** but also in the left lower neck **(H, arrow)**, which is negative on ^{18}F -FDG PET/CT image **(D, arrow)**. Maximum intensity projection ^{68}Ga -FAPI PET/CT image depicts four bone metastases in the thoracic spine, lumbar spine, and left iliac bone **(E, arrows)**, whereas maximum intensity projection ^{18}F -FDG PET/CT image only depicts two lesions in the thoracic and lumbar spine with much lower tracer uptake **(A, arrows)** (Reprinted, with permission, from reference 27.)

- Lindner T, Loktev A, Altmann A, et al. Development of quinoline-based theranostic ligands for the targeting of fibroblast activation protein. *J Nucl Med* 2018;59(9):1415–1422.
- Giesel FL, Kratochwil C, Lindner T, et al. ^{68}Ga -FAPI PET/CT: Biodistribution and Preliminary Dosimetry Estimate of 2 DOTA-Containing FAP-Targeting Agents in Patients with Various Cancers. *J Nucl Med* 2019;60(3):386–392.
- Loktev A, Lindner T, Burger EM, et al. Development of Fibroblast Activation Protein-Targeted Radiotracers with Improved Tumor Retention. *J Nucl Med* 2019;60(10):1421–1429.
- Millul J, Bassi G, Mock J, et al. An ultra-high-affinity small organic ligand of fibroblast activation protein for tumor-targeting applications. *Proc Natl Acad Sci U S A* 2021;118(16):e2101852118.
- Backhaus P, Gierse F, Burg MC, et al. Translational imaging of the fibroblast activation protein (FAP) using the new ligand [^{68}Ga]Ga-OncoFAP-DOTAGA. *Eur J Nucl Med Mol Imaging* 2022;49(6):1822–1832.
- Giesel FL, Adeberg S, Syed M, et al. FAPI-74 PET/CT using either ^{18}F -AlF or cold-kit ^{68}Ga labeling: biodistribution, radiation dosimetry, and tumor delineation in lung cancer patients. *J Nucl Med* 2021;62(2):201–207.
- Giesel FL, Kratochwil C, Schlittenhardt J, et al. Head-to-head intra-individual comparison of biodistribution and tumor uptake of ^{68}Ga -FAPI and ^{18}F -FDG PET/CT in cancer patients. *Eur J Nucl Med Mol Imaging* 2021;48(13):4377–4385.
- Kratochwil C, Flechsig P, Lindner T, et al. ^{68}Ga -FAPI PET/CT: Tracer Uptake in 28 Different Kinds of Cancer. *J Nucl Med* 2019;60(6):801–805.
- Dendl K, Koerber SA, Finck R, et al. ^{68}Ga -FAPI-PET/CT in patients with various gynecological malignancies. *Eur J Nucl Med Mol Imaging* 2021;48(12):4089–4100.
- Chen H, Pang Y, Wu J, et al. Comparison of [^{68}Ga]Ga-DOTA-FAPI-04 and [^{18}F] FDG PET/CT for the diagnosis of primary and metastatic lesions in patients with various types of cancer. *Eur J Nucl Med Mol Imaging* 2020;47(8):1820–1832.
- Zhao L, Pang Y, Luo Z, et al. Role of [^{68}Ga]Ga-DOTA-FAPI-04 PET/CT in the evaluation of peritoneal carcinomatosis and comparison with [^{18}F] FDG PET/CT. *Eur J Nucl Med Mol Imaging* 2021;48(6):1944–1955.
- Wang H, Zhu W, Ren S, et al. ^{68}Ga -FAPI-04 versus ^{18}F -FDG PET/CT in the detection of hepatocellular carcinoma. *Front Oncol* 2021;11:693640.
- Shi X, Xing H, Yang X, et al. Comparison of PET imaging of activated fibroblasts and ^{18}F -FDG for diagnosis of primary hepatic tumours: a prospective pilot study. *Eur J Nucl Med Mol Imaging* 2021;48(5):1593–1603.
- Guo W, Pang Y, Yao L, et al. Imaging fibroblast activation protein in liver cancer: a single-center post hoc retrospective analysis to compare [^{68}Ga] Ga-FAPI-04 PET/CT versus MRI and [^{18}F] FDG PET/CT. *Eur J Nucl Med Mol Imaging* 2021;48(5):1604–1617.
- Kuten J, Levine C, Shamni O, et al. Head-to-head comparison of [^{68}Ga]Ga-FAPI-04 and [^{18}F] FDG PET/CT in evaluating the extent of disease in gastric adenocarcinoma. *Eur J Nucl Med Mol Imaging* 2022;49(2):743–750.
- Qin C, Shao F, Gai Y, et al. ^{68}Ga -DOTA-FAPI-04 PET/MR in the evaluation of gastric carcinomas: Comparison with ^{18}F -FDG PET/CT. *J Nucl Med* 2022;63(1):81–88.

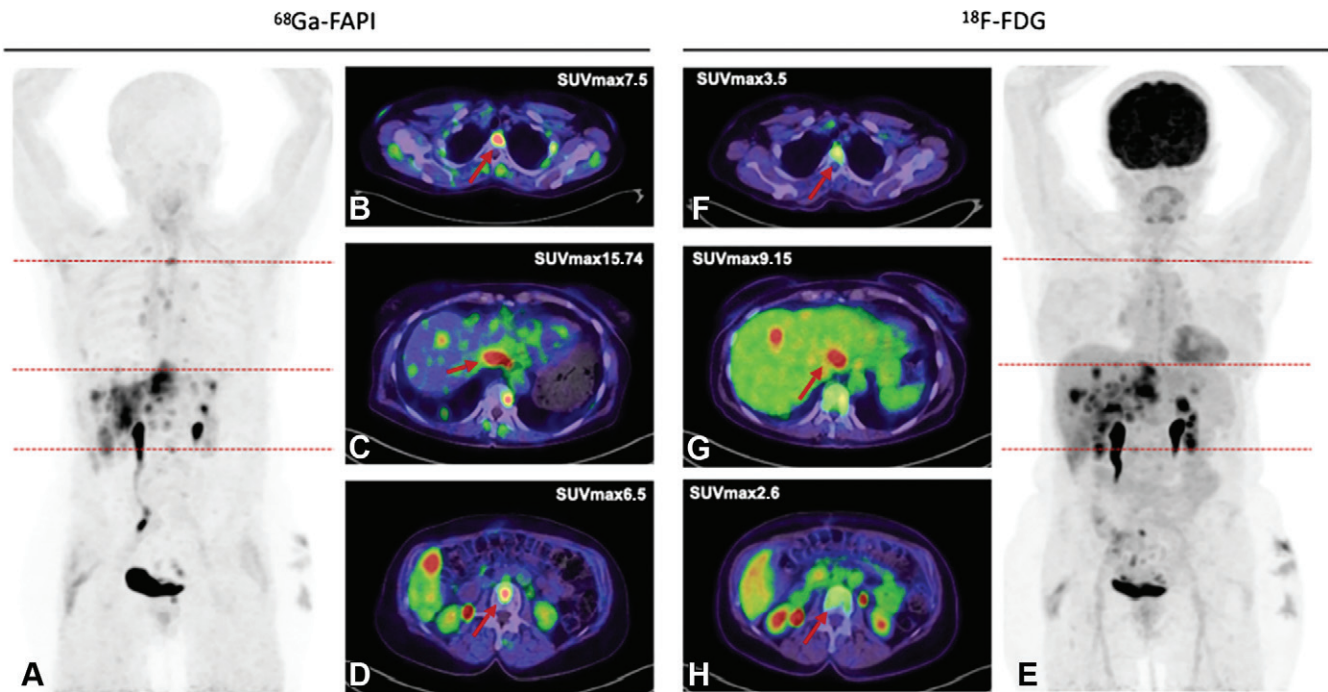


Figure 10: Images in a 63-year-old woman with metastasized ovarian carcinoma who underwent gallium 68 (^{68}Ga)-labeled fibroblast activation protein inhibitor (FAP) PET/CT (left images) followed by fluorine 18 (^{18}F) fluorodeoxyglucose (FDG) PET/CT (right images) 1 month later. (**A, E**) Anterior maximum intensity projection images from ^{68}Ga -FAP PET (**A**) and ^{18}F -FDG PET (**E**). (**B–D, F–H**) Axial fused PET/CT images depict bone metastases in the upper thoracic spine (**B, F**; arrow) and the lower thoracic spine (**D, H**; arrow) and a liver metastasis in segment I (**C, G**; arrow) with a rather high FAPI uptake (left images) compared with FDG (right images) (maximum standardized uptake value [SUV_{max}] of FAPI vs FDG: 7.5 vs 3.5, respectively, in the bone metastasis in the upper thoracic spine, 6.5 vs 2.6 in the bone metastasis in the lower thoracic spine, and 15.7 vs 9.2 in the liver metastasis). (Adapted, under a CC BY license, from reference 13.)

- Zhao L, Chen S, Chen S, et al. ^{68}Ga -fibroblast activation protein inhibitor PET/CT on gross tumour volume delineation for radiotherapy planning of oesophageal cancer. *Radiother Oncol* 2021;158:55–61.
- Ristau J, Giesel FL, Haefner MF, et al. Impact of Primary Staging with Fibroblast Activation Protein Specific Enzyme Inhibitor (FAP)-PET/CT on Radio-Oncologic Treatment Planning of Patients with Esophageal Cancer. *Mol Imaging Biol* 2020;22(6):1495–1500.
- Koerber SA, Staudinger F, Kratochwil C, et al. The Role of ^{68}Ga -FAP PET/CT for Patients with Malignancies of the Lower Gastrointestinal Tract: First Clinical Experience. *J Nucl Med* 2020;61(9):1331–1336.
- Pang Y, Zhao L, Luo Z, et al. Comparison of ^{68}Ga -FAP and ^{18}F -FDG Uptake in Gastric, Duodenal, and Colorectal Cancers. *Radiology* 2021;298(2):393–402.
- Pang Y, Zhao L, Shang Q, et al. Positron emission tomography and computed tomography with [^{68}Ga]Ga-fibroblast activation protein inhibitors improves tumor detection and staging in patients with pancreatic cancer. *Eur J Nucl Med Mol Imaging* 2022;49(4):1322–1337.
- Giesel FL, Heussel CP, Lindner T, et al. FAP-PET/CT improves staging in a lung cancer patient with cerebral metastasis. *Eur J Nucl Med Mol Imaging* 2019;46(8):1754–1755.
- Wang L, Tang G, Hu K, et al. Comparison of ^{68}Ga -FAP and ^{18}F -FDG PET/CT in the Evaluation of Advanced Lung Cancer. *Radiology* 2022;303(1):191–199.
- Novruzov E, Dendl K, Ndllovu H, et al. Head-to-head intra-individual comparison of [^{68}Ga]-FAP and [^{18}F]-FDG PET/CT in patients with bladder cancer. *Mol Imaging Biol* 2022;24(4):651–658.
- Kömek H, Can C, Güzel Y, et al. ^{68}Ga -FAP-04 PET/CT, a new step in breast cancer imaging: a comparative pilot study with the ^{18}F -FDG PET/CT. *Ann Nucl Med* 2021;35(6):744–752.
- Elboga U, Sahin E, Kus T, et al. Superiority of ^{68}Ga -FAP PET/CT scan in detecting additional lesions compared to ^{18}F -FDG PET/CT scan in breast cancer. *Ann Nucl Med* 2021;35(12):1321–1331.
- Koerber SA, Finck R, Dendl K, et al. Novel FAP ligands enable improved imaging contrast in sarcoma patients due to FAP-PET/CT. *Eur J Nucl Med Mol Imaging* 2021;48(12):3918–3924.
- Kessler L, Ferdinandus J, Hirmas N, et al. ^{68}Ga -FAP as a Diagnostic Tool in Sarcoma: Data from the ^{68}Ga -FAP PET Prospective Observational Trial. *J Nucl Med* 2022;63(1):89–95.
- Röhrich M, Loktev A, Wefers AK, et al. IDH-wildtype glioblastomas and grade III/IV IDH-mutant gliomas show elevated tracer uptake in fibroblast activation protein-specific PET/CT. *Eur J Nucl Med Mol Imaging* 2019;46(12):2569–2580.
- Windisch P, Röhrich M, Regnery S, et al. Fibroblast Activation Protein (FAP) specific PET for advanced target volume delineation in glioblastoma. *Radiother Oncol* 2020;150:159–163.
- Qin C, Liu F, Huang J, et al. A head-to-head comparison of ^{68}Ga -DOTA-FAP-04 and ^{18}F -FDG PET/MR in patients with nasopharyngeal carcinoma: a prospective study. *Eur J Nucl Med Mol Imaging* 2021;48(10):3228–3237.
- Syed M, Flechsig P, Liermann J, et al. Fibroblast activation protein inhibitor (FAP) PET for diagnostics and advanced targeted radiotherapy in head and neck cancers. *Eur J Nucl Med Mol Imaging* 2020;47(12):2836–2845.
- Gu B, Xu X, Zhang J, et al. The Added Value of ^{68}Ga -FAP PET/CT in Patients with Head and Neck Cancer of Unknown Primary with ^{18}F -FDG-Negative Findings. *J Nucl Med* 2022;63(6):875–881.
- Kessel K, Seifert R, Weckesser M, et al. Prostate-specific membrane antigen and fibroblast activation protein distribution in prostate cancer: preliminary data on immunohistochemistry and PET imaging. *Ann Nucl Med* 2022;36(3):293–301.
- Jin X, Wei M, Wang S, et al. Detecting Fibroblast Activation Proteins in Lymphoma Using ^{68}Ga -FAP PET/CT. *J Nucl Med* 2022;63(2):212–217.
- Elboga U, Sahin E, Cayirli YB, et al. Comparison of [^{68}Ga]-FAP PET/CT and [^{18}F]-FDG PET/CT in Multiple Myeloma: Clinical Experience. *Tomography* 2022;8(1):293–302.
- Kratochwil C, Giesel FL, Rathke H, et al. [^{153}Sm]Samarium-labeled FAP-46 radioligand therapy in a patient with lung metastases of a sarcoma. *Eur J Nucl Med Mol Imaging* 2021;48(9):3011–3013.
- Lindner T, Altmann A, Krämer S, et al. Design and Development of $^{99\text{m}}\text{Tc}$ -Labeled FAP Tracers for SPECT Imaging and ^{188}Re Therapy. *J Nucl Med* 2020;61(10):1507–1513.

43. Watabe T, Liu Y, Kaneda-Nakashima K, et al. Theranostics Targeting Fibroblast Activation Protein in the Tumor Stroma: ⁶⁴Cu- and ²²⁵Ac-Labeled FAPI-04 in Pancreatic Cancer Xenograft Mouse Models. *J Nucl Med* 2020;61(4):563–569.
44. Varasteh Z, Mohanta S, Robu S, et al. Molecular Imaging of Fibroblast Activity After Myocardial Infarction Using a ⁶⁸Ga-Labeled Fibroblast Activation Protein Inhibitor, FAPI-04. *J Nucl Med* 2019;60(12):1743–1749.
45. Notohamiprodjo S, Nekolla SG, Robu S, et al. Imaging of cardiac fibroblast activation in a patient after acute myocardial infarction using ⁶⁸Ga-FAPI-04. *J Nucl Cardiol* 2022;29(5): 2254–2261.
46. Conen P, Pennetta F, Dendl K, et al. [⁶⁸ Ga]Ga-FAPI uptake correlates with the state of chronic kidney disease. *Eur J Nucl Med Mol Imaging* 2022;49(10):3365–3372.
47. Ferreira C, Rosenkrans Z, Bernau K, et al. Targeting Activated Fibroblasts for non-invasive detection of Lung Fibrosis. *J Nucl Med* 2021;62(supplement 1):10. https://jnm.snmjournals.org/content/62/supplement_1/10.
48. Telo S, Farolfi A, Castellucci P, et al. A case of [⁶⁸Ga]Ga-FAPI-46-avid and [¹⁸F]F-FDG-negative COVID-19 pneumonia sequelae. *Eur J Nucl Med Mol Imaging* 2022;49(7):2452–2453.
49. Levy MT, McCaughan GW, Abbott CA, et al. Fibroblast activation protein: a cell surface dipeptidyl peptidase and gelatinase expressed by stellate cells at the tissue remodelling interface in human cirrhosis. *Hepatology* 1999;29(6):1768–1778.
50. Rovedatti L, Di Sabatino A, Knowles CH, et al. Fibroblast activation protein expression in Crohn's disease strictures. *Inflamm Bowel Dis* 2011;17(5):1251–1253.
51. Gu B, Xu X, Zhang J, et al. The Added Value of ⁶⁸Ga-FAPI-04 PET/CT in Patients with Head and Neck Cancer of Unknown Primary with ¹⁸F-FDG Negative Findings. *J Nucl Med* 2022;63(6):875–881.
52. Liermann J, Syed M, Ben-Josef E, et al. Impact of FAPI-PET/CT on Target Volume Definition in Radiation Therapy of Locally Recurrent Pancreatic Cancer. *Cancers (Basel)* 2021;13(4):796.
53. Röhrich M, Naumann P, Giesel FL, et al. Impact of ⁶⁸Ga-FAPI PET/CT Imaging on the Therapeutic Management of Primary and Recurrent Pancreatic Ductal Adenocarcinomas. *J Nucl Med* 2021;62(6):779–786.
54. Dendl K, Finck R, Giesel FL, et al. FAP imaging in rare cancer entities—first clinical experience in a broad spectrum of malignancies. *Eur J Nucl Med Mol Imaging* 2022;49(2):721–731.
55. Chen H, Zhao L, Ruan D, et al. Usefulness of [⁶⁸Ga]Ga-DOTA-FAPI-04 PET/CT in patients presenting with inconclusive [¹⁸F]FDG PET/CT findings. *Eur J Nucl Med Mol Imaging* 2021;48(1):73–86.
56. Lan L, Zhang S, Xu T, et al. Prospective Comparison of ⁶⁸Ga-FAPI versus ¹⁸F-FDG PET/CT for Tumor Staging in Biliary Tract Cancers. *Radiology* 2022;304(3):648–657.
57. Lindner T, Altmann A, Giesel F, et al. ¹⁸F-labeled tracers targeting fibroblast activation protein. *EJNMMI Radiopharm Chem* 2021;6(1):26.
58. Ballal S, Yadav MP, Moon ES, et al. First-In-Human Results on the Biodistribution, Pharmacokinetics, and Dosimetry of [¹⁷⁷Lu]Lu-DOTA.SA.FAPi and [¹⁷⁷Lu]Lu-DOTAGA.(SA.FAPi)₂. *Pharmaceuticals (Basel)* 2021;14(12):1212.
59. Aertgeerts K, Levin I, Shi L, et al. 1Z68: Crystal Structure Of Human Fibroblast Activation Protein alpha. *Worldwide Protein Data Bank*. . Published April 12, 2005. Revised July 13, 2011.
60. Nar H, Schnapp G, Schreiner P. 6Y0F: Structure of human FAPalpha in complex with linagliptin. *Worldwide Protein Data Bank*. Published February 17, 2021.
61. Jansen K, Heirbaut L, Cheng JD, et al. Selective Inhibitors of Fibroblast Activation Protein (FAP) with a (4-Quinolinoyl)-glycyl-2-cyanopyrrolidine Scaffold. *ACS Med Chem Lett* 2013;4:491–496.